




## PAPER

[View Article Online](#)  
[View Journal](#) | [View Issue](#)Cite this: *Mater. Adv.*, 2025,  
6, 2365

# Synthesis of gold nanoparticles using *Eutrema japonicum* (Wasabi): antioxidant and anti-inflammatory studies†

Christian Nanga Chick, \*<sup>ab</sup> Mahiro Takano,<sup>a</sup> Francois Eya'ane Meva <sup>b</sup> and  
Toyonobu Usuki \*<sup>a</sup>

In this study, gold nanoparticles with *Eutrema japonicum* (AuNPs-E.j.) were synthesized using the butylene glycol extract of the plant's grated stem and Au(III) chloride trihydrate solution. The primary characterization of synthesized AuNPs-E.j. using a UV-Vis spectrometer indicated the presence of a surface plasmon resonance band between 500 and 600 nm, indicating the reduction of Au(III) to Au(0). Infrared spectroscopy revealed the existence of C–O, OH, C–H, C=O, and C–C vibrations or stretching along with aliphatic hydrocarbon chains of as-synthesized AuNP-E.j. Dynamic light scattering indicated an average particle size of 35.94 nm and a zeta potential value of 3.53 mV. AuNPs-E.j. reduced 1,1-diphenyl-2-picrylhydrazyl and phosphomolybdenum radicals, with ascorbic acid equivalent antioxidant capacity of 1.08 and 24.63 mg/100 mL, respectively. In addition, the albumin denaturation inhibitory activity of AuNPs-E.j. was equivalent to a percentage inhibition value of the standard drug (diclofenac) value (0.36 mg/100 mL). This study confirmed that AuNPs-E.j. have the potential as a therapeutic agent for treating oxidative stress, inflammatory problems and related diseases.

Received 25th January 2025,  
Accepted 5th March 2025

DOI: 10.1039/d5ma00065c

[rsc.li/materials-advances](https://rsc.li/materials-advances)

## Introduction

Plant *Eutrema japonicum* (E.j.) (*syn. Wasabia japonica*), commonly known as 'Wasabi' or 'Japanese horseradish' belongs to the Brassicaceae family and is native to Japan. Its stem is ground into a paste that serves as a pungent condiment for the consumption of 'sushi' and other foods. The fresh paste has a distinct flavor and stimulates the nose,<sup>1</sup> with allyl isothiocyanate as the volatile compound responsible for its initial pungency. This compound is formed by the hydrolysis of allyl glucosinolate, a natural thioglucoside. When the plant is grated, cell rupture results in the release of myrosinase, which catalyzes hydrolysis.<sup>1,2</sup> As a protective mechanism, the plant releases allyl isothiocyanate when damaged.<sup>3</sup>

Such plants contain numerous complex chemicals derived from the hydrolysis of thioglucosides, including sinigrin and other glucosinolates, yielding glucose and methylthioalkyl isothiocyanates [6-(methyl sulfinyl)hexyl isothiocyanate, 7-methyl thio-heptyl isothiocyanate, and 8-methylthiooctyl isothiocyanate].<sup>1–5</sup> These

isothiocyanates inhibit microbial growth, preserve food against spoilage, and suppress oral bacterial growth.<sup>6</sup> In addition, the Wasabi plant is rich in carotenoids and flavonoids (isovitexin 4'-O-glucoside, luteolin 3',7'-diglucoside, kaempferol 3-O-rutinoside, and phenylpropanoids).<sup>7–11</sup> Extracts of the leaves and roots of E.j. exhibit anti-inflammatory, anti-neuroinflammatory, antigenotoxic, antioxidant, anticancer, neuroprotective, and antiobesity properties.<sup>10–16</sup>

Recently, Katarzyna *et al.* performed LC-DAD-IT-MS and LC-QTOF-MS analyses of the leaf and root extracts of Wasabi, revealing the presence of 42 constituents, including glucosinolates, phenylpropanoid glycosides, flavone glycosides, and hydroxycinnamic acids. The extracts were assessed for their potential cytotoxic effect on human colon adenocarcinoma cells, effects on the growth of probiotic and intestinal pathogenic strains, and their anti-inflammatory properties. The ethanol extract, obtained from the biennial roots, exhibited the most potent effects compared to other samples.<sup>17</sup>

Developing new environmentally friendly solvents to replace conventional organic solvents is crucial for advancing green extraction techniques.<sup>18</sup> However, conventional solvents have limitations, including time, cost, and energy consumption for the separation of organic solvents from extracts. To overcome these limitations, solvents such as butanediol or butylene glycol (BG; 1,3-BG was used in this study) can be used for plant extraction. These solvents are widely used in cosmetic and

<sup>a</sup> Department of Materials and Life Sciences, Faculty of Science and Technology, Sophia University, 7-1 Kioicho, Chiyoda-ku, Tokyo 102-8554, Japan.

E-mail: [chicknanga0@gmail.com](mailto:chicknanga0@gmail.com), [t-usuki@sophia.ac.jp](mailto:t-usuki@sophia.ac.jp)

<sup>b</sup> Laboratory of Innovative Nanostructured Material (NANO: C), Faculty of Medicine and Pharmaceutical Sciences, The University of Douala, B.P. 2701, Cameroon

† Electronic supplementary information (ESI) available. See DOI: <https://doi.org/10.1039/d5ma00065c>

pharmaceutical formulations without being removed from the extract and are categorized as a safe chemical and flavor molecule by the United States Food and Drug Administration (FDA). BG is detected in some bell peppers and is typically administered to stimulate the biosynthesis of  $\beta$ -hydroxybutyrate, a ketone body linked to healthy benefits.<sup>19</sup> BG is used as a hypoglycaemic agent, intermediate in manufacture of polyester plasticizers; humectant for cellophane, tobacco and has some mould inhibiting action.<sup>20</sup>

Green nanotechnology focuses on synthesis using natural sources such as plants, bacteria, and fungi, which are safer for the environment and humans.<sup>21,22</sup> Researchers have intensively screened molecules that can reduce metallic ions, such as Ag, Au, and Fe, to their reduced ions. Gold nanoparticles (AuNPs) have various applications owing to their surface plasmon resonance (SPR), size- and shape-dependent properties, and biocompatibility.<sup>23</sup> The pioneering work of Turkevich *et al.* marked a significant milestone in AuNP synthesis, leading to diverse modified and improved methods.<sup>24</sup> However, the synthesis of AuNPs remains a complex research area that involves controlling various parameters such as particle size, charge, elemental composition and several physico-chemical factors, particularly the temperature gradient, efficiency of reagent mixing, and resulting local concentration gradient.

This study explored the application of E.j. BG extract (BG-E.j.) as a reducing or capping agent for synthesizing metallic AuNPs. To our knowledge, this is the first study that used “Wasabi” for the synthesis of metal NPs. The synthesized AuNPs were characterized and evaluated for their antioxidant capacity, such as phosphomolybdenum and 1,1-diphenyl picrylhydrazyl (DPPH). In addition, their albumin denaturation activity was examined to validate their therapeutic application scope.

## Results and discussion

E.j. Wasabi (Fig. S1, ESI<sup>†</sup>) was purchased from Daio Wasabi Nozjo (Nagano, Japan). A grated paste (30 g) was added to 100 mL of the prepared 30% BG solution for extraction, followed by centrifugation and filtration. A 5 mM Au(III) chloride trihydrate ( $\text{HAuCl}_4 \cdot 3\text{H}_2\text{O}$ ) solution was prepared. Three samples (Fig. S2,

ESI<sup>†</sup>) were prepared as follows: control sample ‘A’ consisting of equal volumes of 30% BG and 5 mM  $\text{HAuCl}_4 \cdot 3\text{H}_2\text{O}$  solution, reference sample ‘B’ consisting of a 0.1% w/v ascorbic acid (A.a.) in 30% BG solution, and test sample consisting of 30% w/v E.j. in 30% BG extract solution. Each mixture was stirred at 1500 rpm and heated at 110 °C for 5 min. A color change was observed in the samples, and UV-Vis spectroscopy was performed (Fig. 1). The prepared AuNP solution was then stored and used for further investigation.

The color of the standard reducing agent (A.a.) changed immediately from yellow to bluish purple upon addition to the  $\text{HAuCl}_4 \cdot 3\text{H}_2\text{O}$  solution, confirming the formation of AuNP-A.a., as previously reported.<sup>25</sup> After vigorous stirring and heating, the color of the samples containing the plant extract or A.a. changed to dark purple with black precipitates. The color of control sample ‘A’ did not change for the entire process (Fig. S2, ESI<sup>†</sup>). The observed color changes in samples B and C were primarily attributed to the SPR phenomenon. SPR occurs when the collective oscillations of free electrons in NPs interact with the electromagnetic field of light. This interaction results in the absorption of light at specific wavelengths, leading to a change in the color of the solution, which serves as a valuable indicator for the successful formation of NPs. Thus, a simple and non-invasive method based on the SPR phenomenon can be developed for monitoring the synthesis of AuNPs.<sup>26</sup>

UV-Vis spectroscopy was performed on the samples at different time intervals; the spectra are shown in Fig. 1. The prepared AuNP samples were measured at time intervals ( $t = 0$  and 6 h) after AuNP synthesis (Fig. S3, ESI<sup>†</sup>). An SPR band within the 500–650 nm range was observed for the AuNP-E.j. and AuNP-A.a. solutions, indicating distinct absorbances for the samples.

The infrared (IR) spectra of the samples were recorded between 4000 and 500  $\text{cm}^{-1}$  (Fig. 2). Intense absorption bands were observed at 3337  $\text{cm}^{-1}$  (OH for alcohol), 2927  $\text{cm}^{-1}$  (C–H for characteristic stretching methyl group), 2358  $\text{cm}^{-1}$  (weak bands of conjugated C=C), 1744  $\text{cm}^{-1}$  (C=O for a conjugate aldehyde or a primary amide), 1368  $\text{cm}^{-1}$  (C–H stretching for the hydrocarbon chain), 1218  $\text{cm}^{-1}$  (C–O bending or phenol group), 1056  $\text{cm}^{-1}$  (C–H), 960  $\text{cm}^{-1}$  (C–H or OH), 905  $\text{cm}^{-1}$

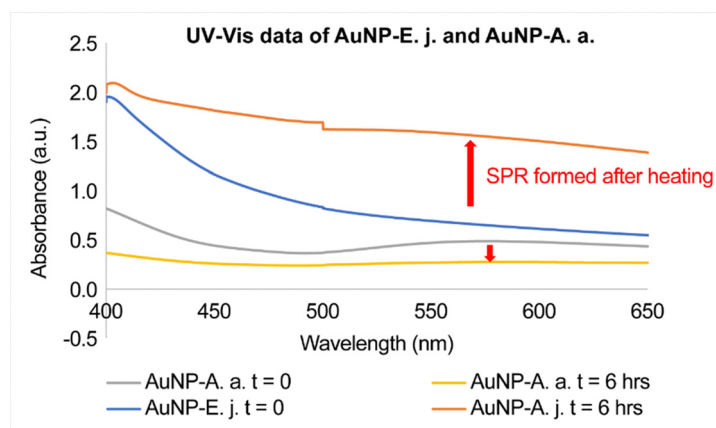


Fig. 1 UV-Vis spectra of the gold nanoparticles (AuNPs) from *E. japonicum* (E.j.) and ascorbic acid (A.a.) (AuNP-E.j. and AuNP-A.a., respectively).



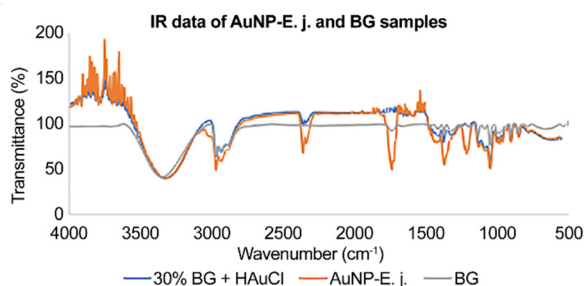


Fig. 2 Infrared spectra of AuNP-E.j. and butylene glycol (BG) samples.

(C–H aromatics), and  $850\text{ cm}^{-1}$  (O–Ag interaction in the produced NPs, the C–Cl stretching in an alkyl group, or the out-of-plane bending vibration of the C–H group).

In the IR spectrum for AuNP-E.j., peaks corresponding to C=C conjugate stretching at  $2358\text{ cm}^{-1}$ , the carboxylic group for the conjugate aldehyde or a primary amide at  $1744\text{ cm}^{-1}$ , hydrocarbon chains for C–H at  $1368$  and  $1056\text{ cm}^{-1}$ , C–O bending for phenol groups, and C–H or O–H rocking along the fingerprint region were more intense than those for the BG sample. The elements or functional groups were derived from the compounds present in E.j. and were responsible for the reduction, capping, or stabilization of the formed AuNPs. Therefore, various compounds are considered responsible for NP synthesis.

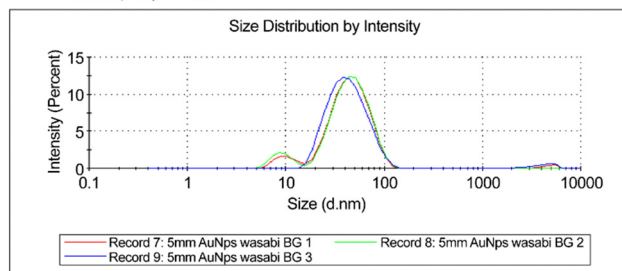
Dynamic light scattering (DLS) results for AuNP-E.j. indicate an average hydrodynamic particle size of  $35.94\text{ nm}$ , and a polydispersity index (PDI) of  $0.285$ , indicating that the samples are suitable for analysis (Fig. 3). According to DLS guidelines, a PDI value of  $<0.1$  indicates high monodispersity, a PDI value between  $0.1$  and  $0.25$  represents a narrow distribution with minimal aggregates, and a PDI value  $>0.25$  indicates polydispersity with significant aggregation. Therefore, AuNP-E.j. were found to be significantly polydispersed and aggregated.

The zeta potential (ZP or  $\zeta$ ) value of AuNP-E.j. was  $3.53\text{ mV}$ . The ZP or electrokinetic potential reflected the potential difference between the electric double layer of the electrophoretic mobile particles and the layer of the dispersant around them in the slipping plane. As a general rule,  $\zeta \geq 30$  and  $\leq 60\text{ mV}$  in the absolute value is considered good and represents excellent stability in that order, while  $\zeta \geq \pm 30\text{ mV}$  indicates monodisperse formulations without aggregates. In contrast,  $\zeta \approx \pm 20\text{ mV}$  is characteristic of short-term stability, while  $\zeta < 5\text{ mV}$  indicates that rapid aggregation in AuNP-E.j.<sup>26</sup>

The ascorbic acid equivalent capacity (AAEC) of the samples to reduce phosphomolybdenum and DPPH was tested. Triplicate serially diluted A.a. solutions at varying concentrations were tested for percentage inhibition, and histograms were plotted for different wavelengths (Fig. S4 and S5, ESI†).

The DPPH radical assay was performed as described previously.<sup>27</sup> The A.a. samples for calibration were prepared at various concentrations ( $125$ – $15.625\text{ }\mu\text{g/mL}$ ). The absorbance of the samples was measured using UV-Vis spectrometry at  $517\text{ nm}$  to calculate percentage inhibition. The percentage inhibition of the sample decreased with decreasing sample concentration. A phosphomolybdenum reduction test was performed as described in our

| Size (d.nm): % Intensity: St Dev (d.nm): |       |         |                  |
|--|-------|---------|------------------|
| Z-Average (d.nm):                        | 35.94 | Peak 1: | 48.71 91.1 19.60 |
| PdI:                                     | 0.285 | Peak 2: | 10.36 7.6 2.548  |
| Intercept:                               | 0.854 | Peak 3: | 4864 14 690.7    |
| Result quality:                          | Good  |         |                  |



| Mean (mV) Area (%) St Dev (mV): |      |         |                 |
|---------------------------------|------|---------|-----------------|
| Zeta Potential (mV):            | 3.53 | Peak 1: | 3.53 100.0 3.86 |
| Zeta Deviation (mV):            | 3.86 | Peak 2: | 0.00 0.0 0.00   |
| Conductivity (mS/cm):           | 2.92 | Peak 3: | 0.00 0.0 0.00   |
| Result quality:                 | Good |         |                 |

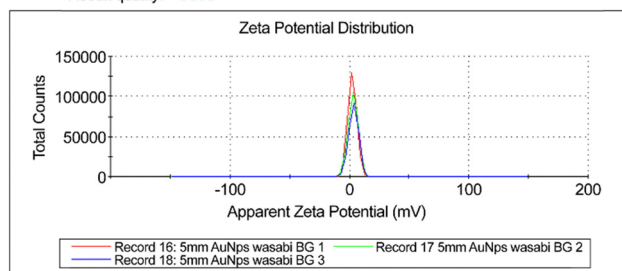


Fig. 3 Hydrodynamic particle size and zeta potential of AuNP-E.j.

previous study.<sup>21,28</sup> A.a. at a concentration of  $250$ – $15.625\text{ }\mu\text{g/mL}$  was used for calibration, and absorbance was measured *via* UV-Vis spectrophotometry at  $695\text{ nm}$  (Fig. 4). Percentage inhibition was calculated by the same method as that reported previously.<sup>27</sup>

For each sample (AuNP-A.a., AuNP-E.j., E.j. extract, and  $\text{HAuCl}_4 \cdot 3\text{H}_2\text{O}/30\%$  BG solution) prepared in triplicate using  $2\text{ mL}$  of the solution, the percentage inhibition per assay was measured. The AAEC for each sample was calculated from calibration equations ( $y = 35.07 \ln(x) - 82.62$ ) and ( $y = 3.97x + 1.17$ ) for the DPPH and molybdenum reduction assays, respectively (Fig. 4).

In the DPPH reduction assay, the AuNP-A.a. exhibited the highest potency, inhibiting the radical or oxidizing agent by  $10.2\%$ . AuNP-A.a., E.j. extract, and AuNP-E.j. exhibited decreasing AAEC values of  $1.41$ ,  $1.12$ , and  $1.08\text{ mg/100 mL}$ , respectively, which were equivalent to that of A.a. For the molybdenum reduction test, the inhibitory effects of the samples were in decreasing order: AuNP-E.j.  $>$  E.j. extract  $>$  AuNP-A.a. For this test, AuNP-E.j. exhibited the highest AAEC value of  $24.63\text{ mg/100 mL}$ , followed by  $23.73$  and  $2.67\text{ mg/100 mL}$  for E.j. extract and AuNP-A.a., respectively.

The heat-induced egg albumin denaturation method, as described in previous reports, was used to measure the anti-inflammatory activity of the prepared samples.<sup>21,22</sup> This method measures the ability of the samples to inhibit protein tertiary or secondary structure disorientation. Diclofenac (a nonsteroidal anti-inflammatory medication) at concentrations ( $100$ ,  $50$ , and  $25\text{ }\mu\text{g/mL}$ ) was used for calibration. Diclofenac inhibits egg



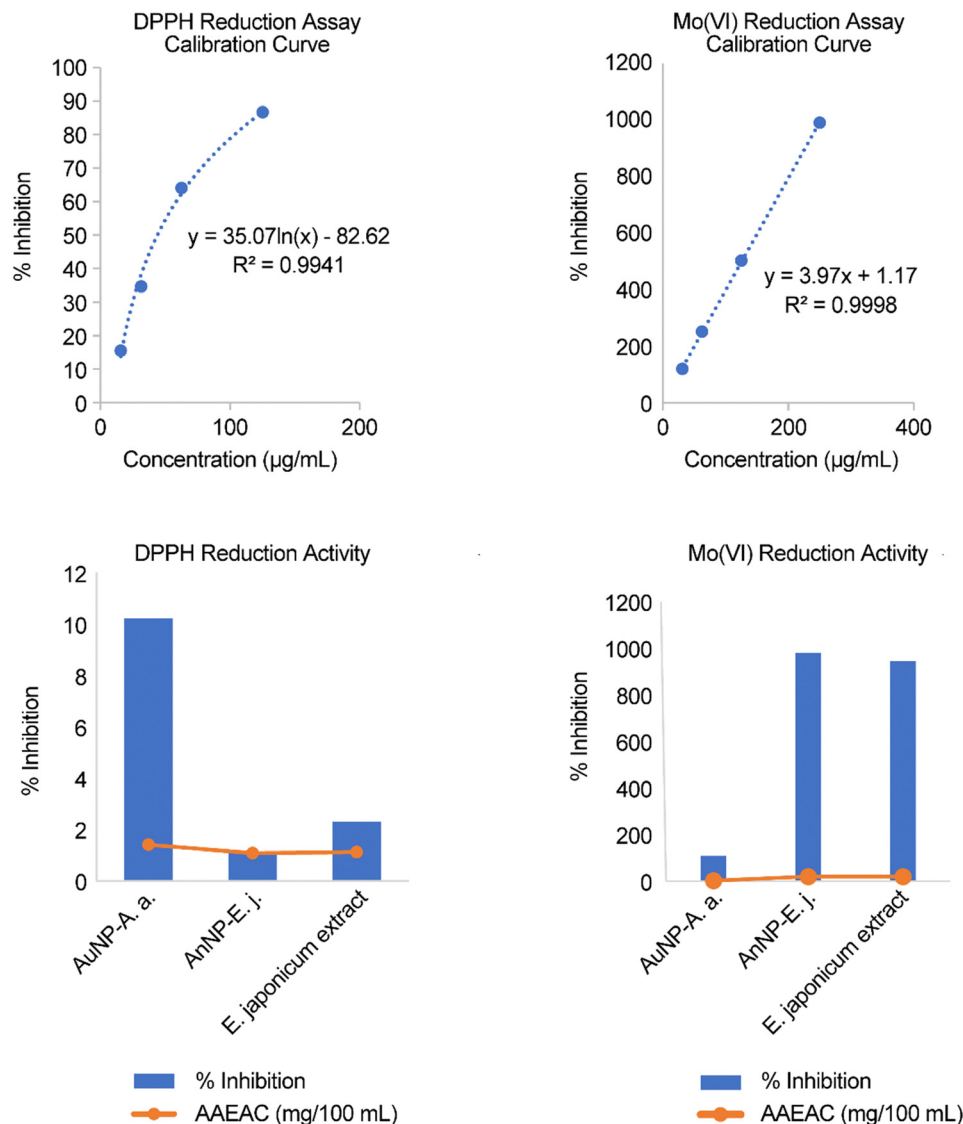


Fig. 4 Calibration curves and DPPH & Mo(vi) reduction capacity for AuNPs and E.j. extract.

albumin denaturation in a concentration-dependent manner (Fig. 5). From the obtained calibration equation,  $y = 31.24\ln x + 13.67$ , the percentage clearance of synthesized AuNP-E.j. was calculated. The diclofenac equivalent albumin denaturation activity of synthesized AuNP-E.j. was 4.5 times higher than the sample without the plant extracts ( $\text{HAuCl}_4 \cdot 3\text{H}_2\text{O}/30\%$  BG solution) (Table 1).

AuNPs have been extensively applied in modern medical and biological studies. AuNPs are used across almost all medical fields, including diagnostics, therapy, prevention, and hygiene. Their unique physical and chemical properties, particularly their optical properties, size, shape, and structure, render them useful. Unlike conventional therapeutic agents, nanoscale drug carriers exhibit enhanced permeability and retention effects.<sup>29</sup> Among the numerous available drug delivery systems, AuNPs are considered leading platforms for numerous therapeutic purposes. In this study, AuNPs synthesized from E.j. were tested for their antioxidant and anti-inflammatory activities for the first time.

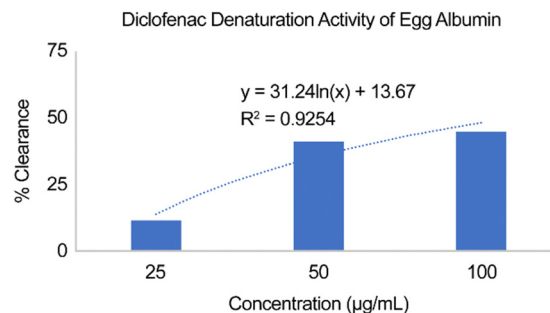


Fig. 5 Diclofenac as control during the calibration of the albumin denaturation test.

As shown in Fig. 4, the DPPH reduction assay reveals excellent percentage inhibition and antioxidant capacity of the AuNP-A.a. and E.j. plant extracts, in that order, in relation to those of AuNP-E.j. However, AuNP-E.j. exhibited superior





**Table 1** Standard drug (diclofenac) equivalent albumin denaturation activity of AuNPs

| Test samples  | Absorbance (A)          | Average A (SD) | Diclofenac equivalent albumin denaturation activity (mg/100 mL) |
|---|-------------------------|----------------|---|
| Control (PBS solution)                                    | —                       | 0.63 (0.130)   | —   |
| AuNP-E.j.   | 0.299<br>0.297<br>0.292 | 0.296 (0.003)  | 0.36  |
| HAuCl <sub>4</sub> ·3H <sub>2</sub> O/<br>30% BG solution | 0.236<br>0.240<br>0.232 | 0.236 (0.004)  | 0.49  |

phosphomolybdenum reduction capacity to E.j. extracts and AuNP-A.a. Therefore, E.j. and AuNP-A.a. are potential antioxidant agents capable of reacting with reactive oxygen, resulting in their elimination or termination.

The inhibition of albumin denaturation by the AuNP-E.j. solution, demonstrating its anti-inflammatory potential, exhibited a slightly lower activity than that by the sample consisting of BG and HAuCl<sub>4</sub>·3H<sub>2</sub>O. Therefore, the phytochemicals present in E.j. such as phenolics, glycosides, terpenoids responsible for the reduction of Au<sup>3+</sup> to Au<sup>0</sup> for the formation of AuNPs were prerequisites for the biological activity of AuNP-E.j.<sup>30</sup> In previous reports, the anti-inflammatory and antioxidant activities of AuNP-E.j. were attributed to the presence of phenolic compounds in the Wasabi extracts.<sup>8</sup> Yoshida *et al.* isolated compounds such as 5-hydroxy ferulic acid methyl ester and all-*trans*-lutein from the methanol leaf extract of Wasabi, which inhibited NO production in murine macrophage cells.<sup>10</sup> A recent clinical trial report showed that the Wasabi extract decreased tyrosinase activity and melanin content and suppressed *in vitro* AGEs formation while improving skin conditions.<sup>31</sup>

BG has the potential to serve as an alternative solvent for plant extracts, as it is widely used in cosmetic and pharmaceutical preparations without being removed from the final extract. In addition, it is categorized as a safe chemical by the United States FDA. BG has been used to extract bioactive compounds from plants such as *Camellia* seed dregs, *Camellia japonica* leaves, and apple waste peel.<sup>32–34</sup> To our knowledge, this study is the first to characterize green-synthesized AuNPs from E.j. and examine their antioxidant and anti-inflammatory properties.

## Conclusions

AuNP-E.j. was synthesized for the first time from the BG-E.j. extract using a green process. Plants Wasabi contain phytochemicals that act as reducing, capping, or stabilizing agents for AuNP formation. Nanometric AuNP-E.j. was charged and aggregated, as confirmed by DLS and particle size and ZP analyses. The antioxidant and anti-inflammatory efficacies of AuNP-E.j. were assessed against free radicals or oxidizing agents to highlight their potency. This study demonstrated the potential pharmaceutical uses of AuNPs produced using a green method as the basis for future novel, effective, and safe antioxidant or anti-inflammatory medications to alleviate age-associated oxidative stress and inflammatory pathologies.

## Data availability

All data generated or analysed during this study are included in this published article and its ESI.†

## Conflicts of interest

There are no conflicts of interest to declare.

## References

- 1 K. Ina, H. Ina, M. Ueda, A. Yagi and I. Kishima, *Agric. Biol. Chem.*, 1989, **53**, 537–538, DOI: [10.1271/bbb1961.53.537](#).
- 2 H. Masuda, Y. Harada, K. Tanaka, M. Nakajima and H. Tabeta, *ACS Symp. Ser.*, 1996, **637**, 67–78, DOI: [10.1021/bk-1996-0637.ch006](#).
- 3 A. Atsumi and T. Saito, *J. Plant Interact.*, 2015, **10**, 152–157, DOI: [10.1080/17429145.2015.1039613](#).
- 4 E. Y. Yu, I. J. Pickering, G. N. George and R. C. Prince, *Biochim. Biophys. Acta, Gen. Subj.*, 2001, **1527**, 156–160, DOI: [10.1016/S0304-4165\(01\)00161-1](#).
- 5 J. Melrose, *Biomedicines*, 2019, **7**, 62, DOI: [10.3390/biomedicines7030062](#).
- 6 Z. Lu, C. R. Dockery, M. Crosby, K. Chavarria, B. Patterson and M. Giedd, *Front. Microbiol.*, 2016, **7**, 1403, DOI: [10.3389/fmicb.2016.01403](#).
- 7 T. Hosoya, Y. S. Yun and A. Kunugi, *Tetrahedron*, 2005, **61**, 7037–7044, DOI: [10.1016/j.tet.2005.04.061](#).
- 8 T. Kurata, N. Misawa, T. Hosoya, T. Yamada-Kato, I. Okunishi and S. Kumazawa, *Food Sci. Technol. Res.*, 2019, **25**, 449–457, DOI: [10.3136/fstr.25.449](#).
- 9 T. Hosoya, Y. S. Yun and A. Kunugi, *Phytochemistry*, 2008, **69**, 827–832, DOI: [10.1016/j.phytochem.2007.08.021](#).
- 10 S. Yoshida, T. Hosoya, S. Inui, H. Masuda and S. Kumazawa, *Food Sci. Technol. Res.*, 2015, **21**, 247–253, DOI: [10.3136/fstr.21.247](#).
- 11 K. Szewczyk, W. Pietrzak, K. Klimek, M. Miazga-Karska, A. Firlej, M. Flisiński and A. Grzywa-Celińska, *Int. J. Mol. Sci.*, 2021, **22**, 6219, DOI: [10.3390/ijms22126219](#).
- 12 A. Lohning, Y. Kidachi, K. Kamiie, K. Sasaki, K. Ryoyama and H. Yamaguchi, *Eur. J. Med. Chem.*, 2021, **216**, 113250, DOI: [10.1016/j.ejmech.2021.113250](#).
- 13 Y. Shimamura, M. Iio, T. Urahira and S. Masuda, *J. Sci. Food Agric.*, 2017, **97**, 2419–2425, DOI: [10.1002/jsfa.8055](#).
- 14 L. Subedi, R. Venkatesan and S. Y. Kim, *Int. J. Mol. Sci.*, 2017, **18**, 1423, DOI: [10.3390/ijms18071423](#).
- 15 M. Yamasaki, T. Ogawa, L. Wang, T. Katsube, Y. Yamasaki, X. Sun and K. Shiwaiku, *Nutr. Res. Pract.*, 2013, **7**, 267–272, DOI: [10.4162/nrp.2013.7.4.267](#).
- 16 J. E. Park, T. H. Lee, S. L. Ham, L. Subedi, S. M. Hong, S. Y. Kim, S. U. Choi, C. S. Kim and K. R. Lee, *Antioxidants*, 2022, **11**, 482, DOI: [10.3390/antiox11030482](#).
- 17 K. Dos Santos Szewczyk, W. Skowrońska, A. Kruk, A. Makuch-Kocka, A. Bogucka-Kocka, M. Miazga-Karska, A. Grzywa-Celińska and S. Granica, *Sci. Rep.*, 2023, **13**, 9142, DOI: [10.1038/s41598-023-36402-y](#).



- 18 J. M. DeSimone, *Science*, 2002, **297**, 799–803, DOI: [10.1126/science.1069622](#).
- 19 C. G. McCarthy, E. W. Waigi, G. Singh, T. R. Castaneda, B. Mell, S. Chakraborty, C. F. Wenceslau and B. Joe, *J. Pharmacol. Exp. Ther.*, 2021, **379**, 245–252, DOI: [10.1124/jpet.121.000796](#).
- 20 *The Merck Index – An Encyclopaedia of Chemicals, Drugs, and Biologicals*, ed. M. J. O'Neil, Royal Society of Chemistry, Cambridge, UK, 2013, p. 276.
- 21 C. N. Chick, F. E. Meva, P. B. E. Kedi and T. Usuki, *Nano Select*, 2024, **6**, e202400093, DOI: [10.1002/nano.202400093](#).
- 22 C. N. Chick, M. Mahdaly, P. B. E. Kedi, K. Sonoko and F. E. Meva, *J. Biomater. Nanobiotechnol.*, 2024, **15**, 25–37, DOI: [10.4236/jbmb.2024.152002](#).
- 23 J. Dong, P. L. Carpinone, G. Pyrgiotakis, P. Demokritou and B. M. Moudgil, *KONA*, 2020, **37**, 224–232, DOI: [10.14356/kona.2020011](#).
- 24 J. Turkevich, P. C. Stevenson and J. Hillier, *Faraday Discuss.*, 1951, **11**, 55, DOI: [10.1039/df9511100055](#).
- 25 L. Malassis, R. Dreyfus, R. J. Murphy, L. A. Hough, B. Donnio and C. B. Murray, *RSC Adv.*, 2016, **6**, 33092–33100, DOI: [10.1039/C6RA00194G](#).
- 26 Z. Németh, I. Csóka, R. Semnani Jazani, B. Sipos, H. Haspel, G. Kozma, Z. Kónya and D. G. Dobó, *Pharmaceutics*, 2022, **14**, 1798, DOI: [10.3390/pharmaceutics14091798](#).
- 27 C. N. Chick, T. Misawa-Suzuki, Y. Suzuki and T. Usuki, *Bioorg. Med. Chem. Lett.*, 2020, **30**, 127526, DOI: [10.1016/j.bmcl.2020.127526](#).
- 28 F. E. Meva, J. O. Mbeng, C. O. Ebongue, C. Schlusener, Ü. Kökam-Demir, A. A. Ntumba, P. B. Kedi, E. Elanga, E. R. N. Loudang, M. H. Nko'o, E. Tchoumbi, V. Deli, C. N. Chick, E. A. Mpondo and C. Janiak, *J. Biomater. Nanobiotechnol.*, 2019, **10**, 102–119, DOI: [10.4236/jbmb.2019.102006](#).
- 29 Y. Nakamura, A. Mochida, P. L. Choyke and H. Kobayashi, *Bioconjug. Chem.*, 2016, **27**, 2225–2238, DOI: [10.1021/acs.bioconjugchem.6b00437](#).
- 30 A. Shah, S. Akhtar, F. Mahmood, S. Urooj, A. B. Siddique, M. I. Irfan, M. Naeem-ul-Hassan, M. Sher, A. Alhoshani, A. Rauf, H. M. A. Amin and A. Abbas, *Surf. Interfaces*, 2024, **51**, 104556, DOI: [10.1016/j.surf.2024.104556](#).
- 31 H.-M. Chiang, J.-L. Lyu, M.-E. Lu, Y.-H. Lin, S.-T. Chan, Y.-K. Lin and C.-F. Chiang, *J. Funct. Foods*, 2023, **100**, 105398, DOI: [10.1016/j.jff.2022.105398](#).
- 32 C.-E. Tsai and L.-H. Lin, *Heliyon*, 2019, **5**, e02315, DOI: [10.1016/j.heliyon.2019.e02315](#).
- 33 T. Mizutani and H. Masaki, *Exp. Dermatol.*, 2014, **23**, 23–26, DOI: [10.1111/exd.12395](#).
- 34 S. Blidi, M. Bikaki, S. Grigorakis, S. Loupassaki and D. P. Makris, *Waste Biomass Valor.*, 2015, **6**, 1125–1133, DOI: [10.1007/s12649-015-9410-3](#).

